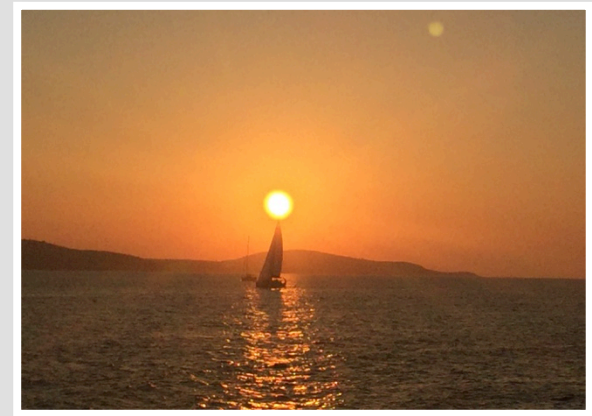


UNRAVELING THE INTERNAL MAGNETIC CONFIGURATION OF THE ICMES



Teresa Nieves-Chinchilla
(GSFC-NASA/CUA)

*'my annual dose of mediterraneo'
Sunset, Sunday Sept 23 (2018)
Picture by me*

ISEST workshop, September 24-28, 2018. Hvar, Croatia.

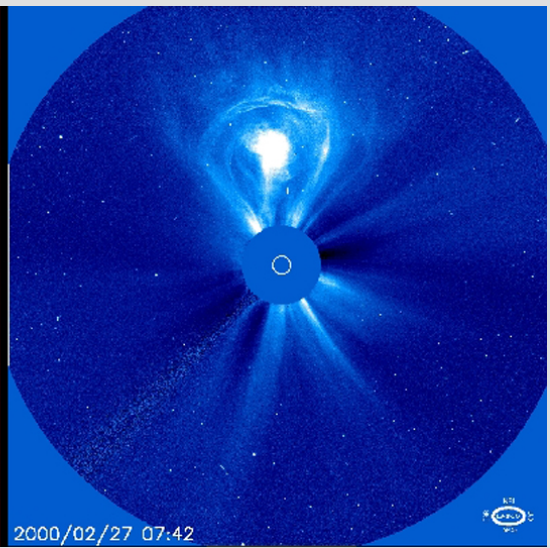
Collaborators: L. Jian (NASA-GSFC), L. Balmaceda (GMU/GSFC), A. Vourlidas (JHU-ApL), M. Linton (NRL), N. Savani (UMBC/GSFC), M.A. Hidalgo (UAH)

HELIOSPHERIC OBSERVATORIES

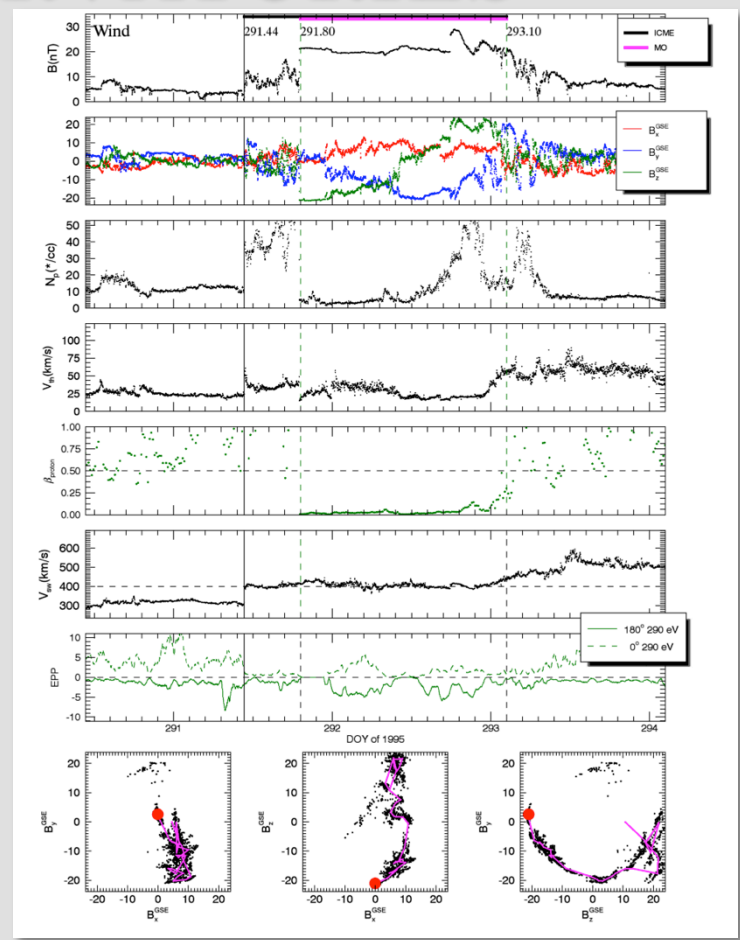
Definition and terminology of ICMEs?

Webb et al. 2012, review

Jian et al 2006
Richardson & Cane, 2006
Zuberchen & Bothmer, 2006

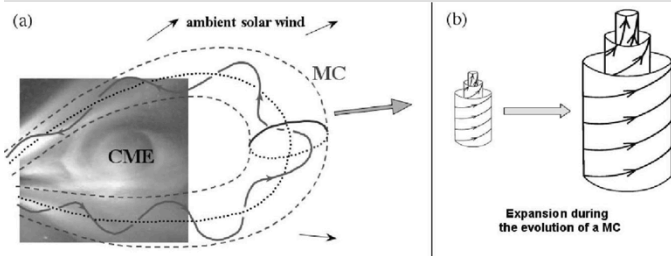


Wind/SWE, MFI

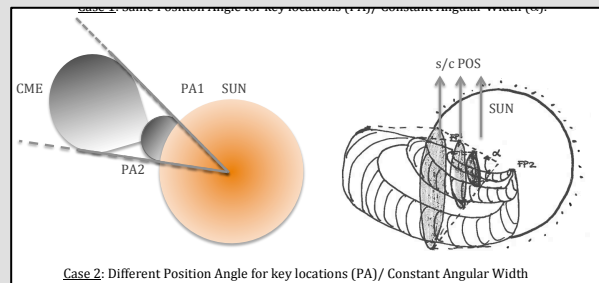


ICME FLUX ROPES - THE THIRD DIMENSION

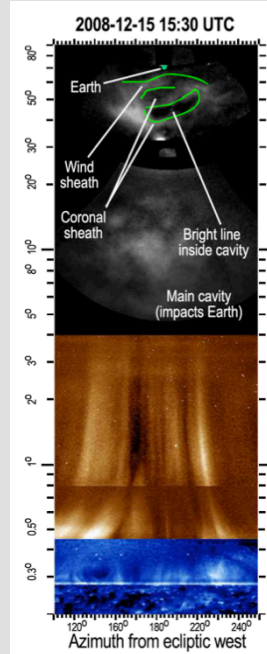
How reliably can we link solar to in situ CME observations?



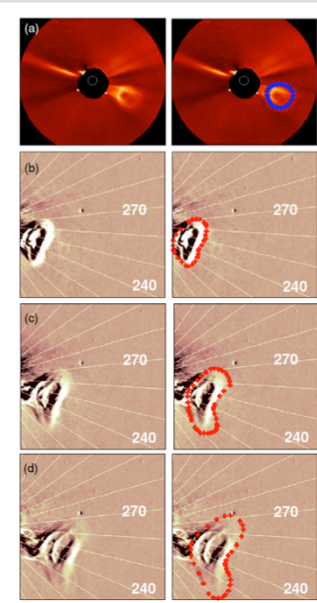
[Dasso et al. 2012, Procc. IAU Symp.]



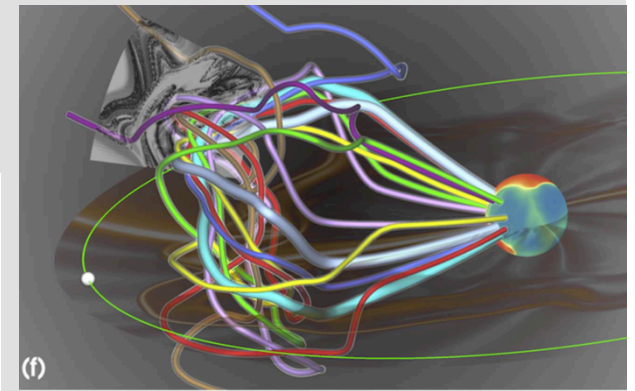
[Nieves-Chinchilla et al. 2012, ApJ.]



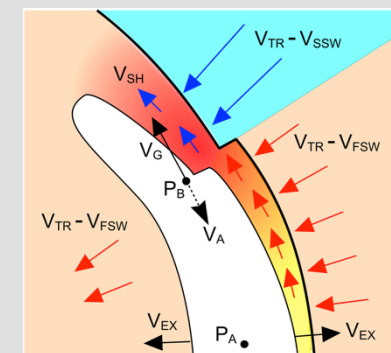
[DeForest et al. 2013, ApJ.]



[Savani et al. 2010, ApJ.]

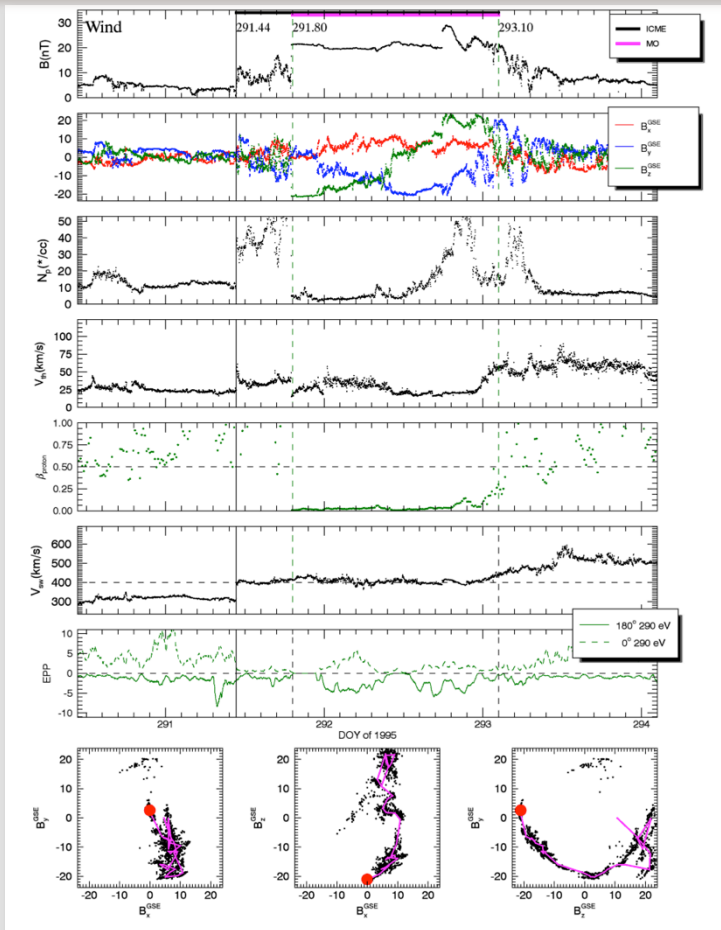


[Torok et al. 2018, ApJ.]



[Owens 2017, NatSR.]

INTERNAL STRUCTURE WITHIN THE ICMES



Magnetic Obstacles (MOs) vs. Magnetic Clouds (MCs)

Magnetic clouds - flux ropes

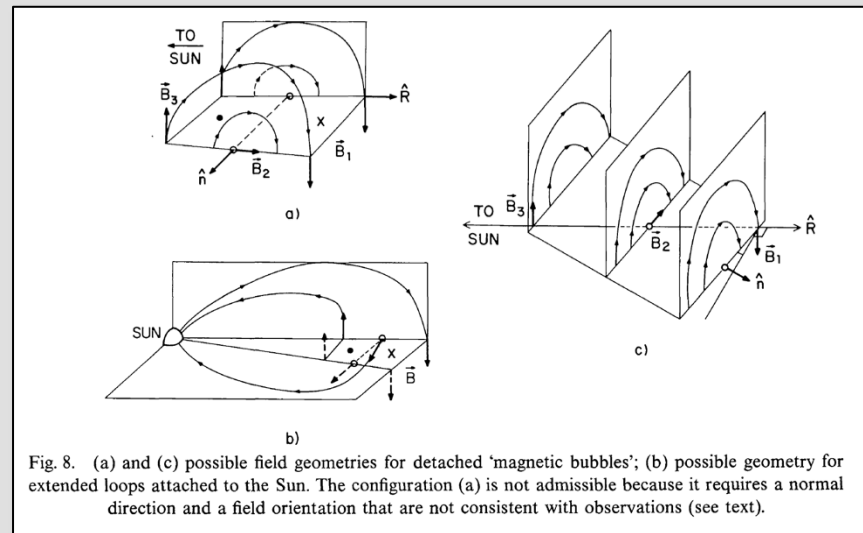
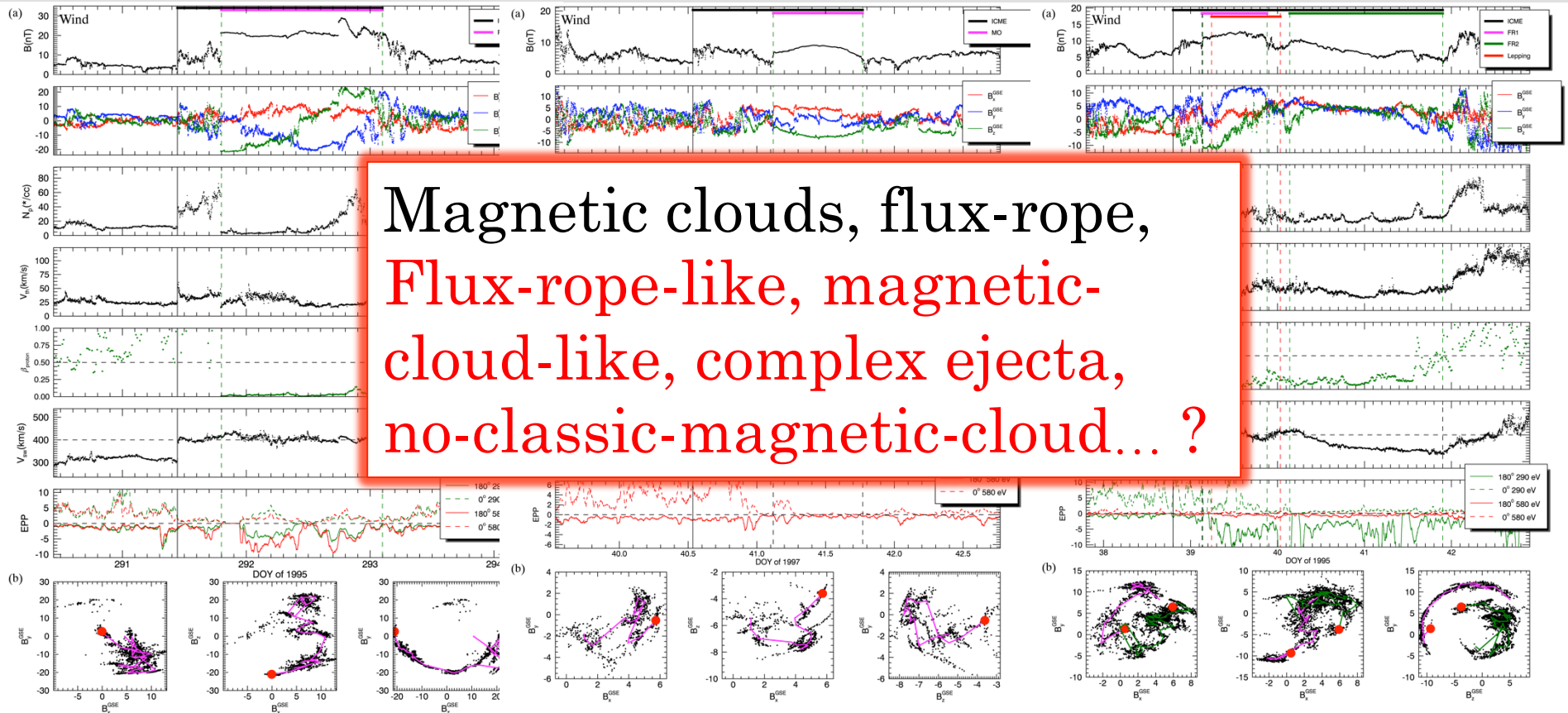


Fig. 8. (a) and (c) possible field geometries for detached 'magnetic bubbles'; (b) possible geometry for extended loops attached to the Sun. The configuration (a) is not admissible because it requires a normal direction and a field orientation that are not consistent with observations (see text).

Burlaga & Behannon, Sol. Phy. 1982.

INTERNAL STRUCTURE WITHIN THE ICMES

MOS Near earth ICMEs – WIND 1995 – 2015 (Nieves-Chinchilla et al. 2018, Sol. Phys.)



QUESTIONS:

- What would be the in-situ mag observations for different s/p trajectories crossing a fR?



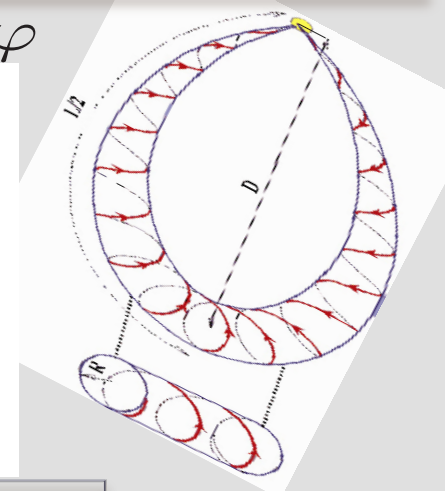
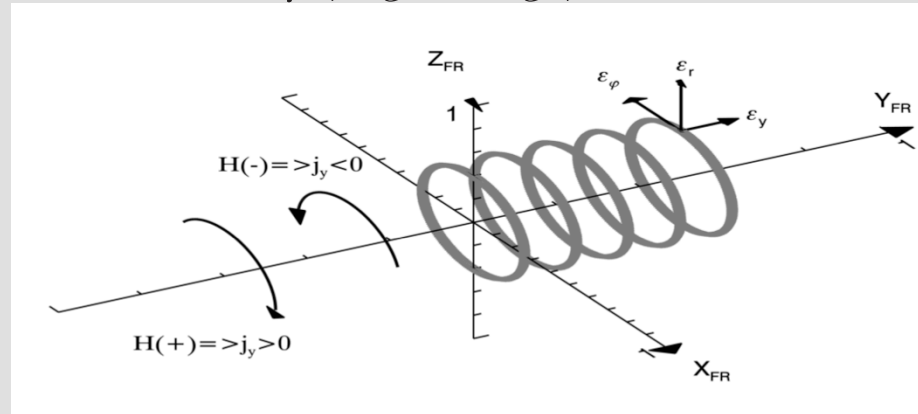
TO-DO LIST:

- ✓ Create synthetic data for all (enough) fR configurations to figure out.

A MODEL FOR HELIOSPHERIC FLUX-ROPES - CIRCULAR

$$x = r \cos \varphi, \quad y = y, \quad z = r \sin \varphi$$

Circular-cylindrical (CC) coordinate system



In this coordinate system, the Maxwell equations, $\nabla \cdot \vec{B} = 0$ and $\nabla \times \vec{B} = \mu_0 \vec{j}$ can be solved under the cylindrical approximation (without radial magnetic field component, $B_r = 0$, and axial invariance, $\partial_y \square = 0$).

$$B_r = 0$$

$$B_y = B_y^0 + \mu_0 \int_0^r j_\varphi(r') dr'$$

$$B_\varphi = -\frac{\mu_0}{r} \int_0^r r' j_y(r') dr'$$

[Nieves-Chinchilla et al. 2016,
Hidalgo et al. 2002]

A MODEL FOR HELIOSPHERIC FLUX-ROPEs - CIRCULAR

Current density components as polynomial functions $B_y^0 = \tau B_n^0 = \tau \frac{\alpha_n}{n+1} R^{n+1}$

$$\vec{j} = (0, \sum_{m=0}^{\infty} \beta_m r^m, -\sum_{n=1}^{\infty} \alpha_n r^n)$$

$$B_r = 0$$

$$B_y = \mu_0 \int_r^R j_\varphi(r') dr'$$

$$B_\varphi = -\frac{\mu_0}{r} \int_0^r r' j_y(r') dr'$$

$$B_r = 0$$

$$B_y = \sum_{n=1}^{\infty} B_n^0 \left[\tau - \left(\frac{r}{R} \right)^{n+1} \right]$$

$$B_\varphi = -\sum_{m=0}^{\infty} \frac{B_n^0}{C_{nm}} \frac{(n+1)}{(m+2)} \left(\frac{r}{R} \right)^{m+1}$$

A MODEL FOR HELIOSPHERIC FLUX-ROPE - CIRCULAR

Current density components as polynomial function

$$\vec{j} = (0, \sum_{m=0}^{\infty} \beta_m r^m, -\sum_{n=1}^{\infty} \alpha_n r^n)$$

Central magnetic field

$$B_r = 0$$

$$B_y = \mu_0 \int_r^R j_\varphi(r') dr'$$

$$B_\varphi = -\frac{\mu_0}{r} \int_0^r r' j_y(r') dr'$$

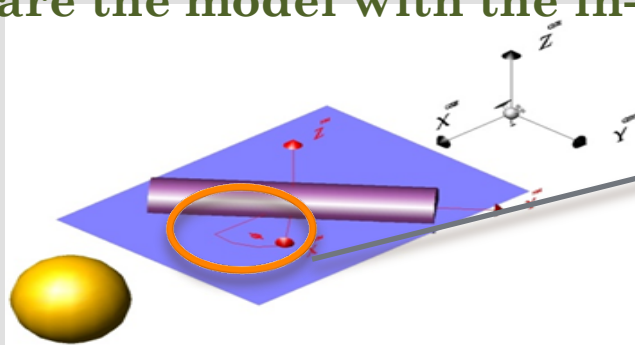
$$D_r = 0$$

$$B_y = \sum_{n=1}^{\infty} B_n^0 \left[\tau - \left(\frac{r}{R} \right)^{n+1} \right]$$

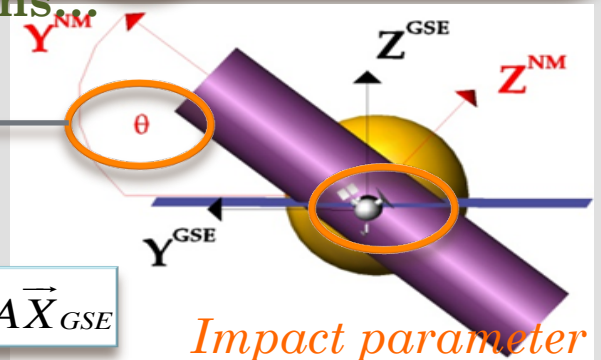
$$B_\varphi = -\sum_{m=0}^{\infty} \frac{B_n^0 (n+1)}{C_{nm} (m+2)} \left(\frac{r}{R} \right)^{m+1}$$

Force-freeness

To compare the model with the in-situ observations,



Orientation

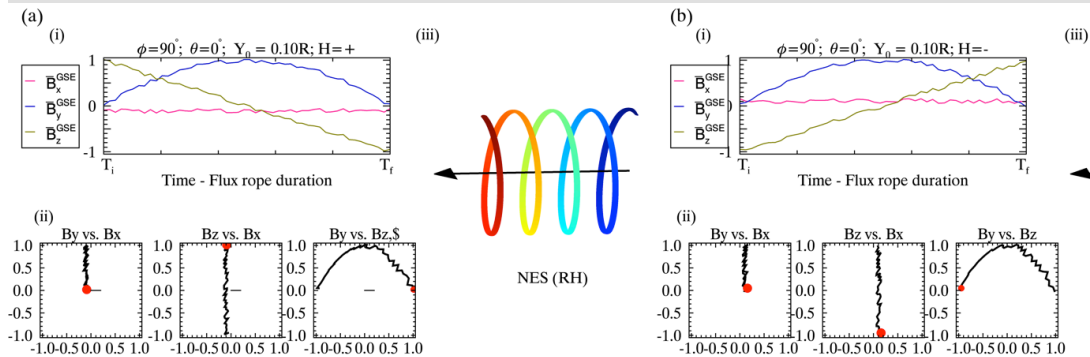


$$\vec{X}^{NM} = \vec{X}_{local} = A \vec{X}^{GSE}$$

Impact parameter

SYNTHETIC DATA OF A VIRTUAL S/P CROSSING A FR

Internal magnetic configuration I (Bothmer & Schwenn, 1998)

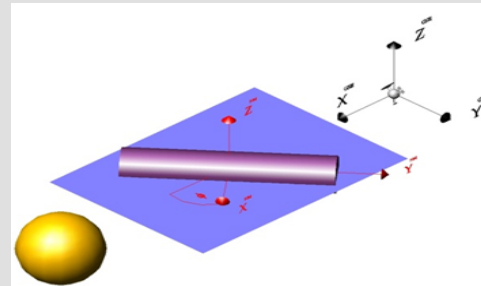


V. Bothmer, R. Schwenn: The structure and origin of magnetic clouds in the solar wind

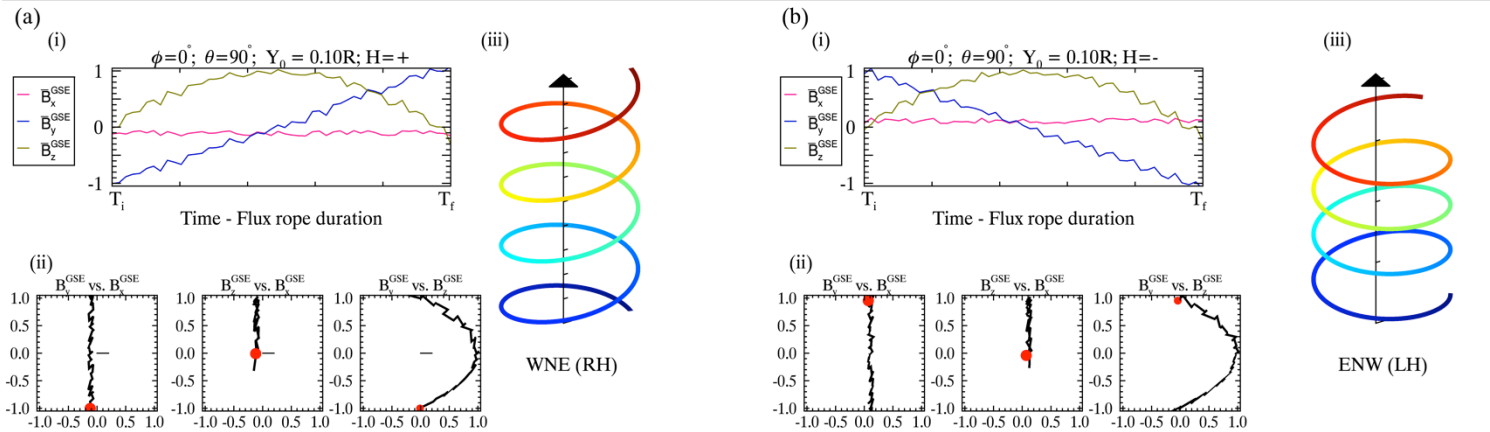
Table 2. Sketch showing the different magnetic configurations of MCs and their magnetic helicity (left-handed (LH), right-handed (RH)) based on the magnetic flux-tube concept and the field relation that a clockwise rotation of the flux-tube axis is the field vector in the B_x - B_y plane.

MC Type	Magnetic helicity	Variation of magnetic field vector	Direction of magnetic field on flux tube axis	Rotation of magnetic field vector in B_x - B_y plane (B_x - B_y plane)
Number of MCs during 1974-1981				
SEN	Left-handed	South (-Bz) → north (+Bz)	East (+By)	
SWN	Right-handed	South (-Bz) → north (+Bz)	West (-By)	
NES	Right-handed	North (+Bz) → south (-Bz)	East (+By)	
NWS	Left-handed	North (+Bz) → south (-Bz)	West (-By)	
Orientations for high inclinations to the ecliptic: SEN, NWS, SWN, NES		East (+By) → west (-By) West (-By) → east (+By)	North (+Bz) → south (-Bz) South (-Bz) → north (+Bz)	Rotations in B_y - B_z (B_y - B_z plane)

BIPOLAR configuration



SYNTHETIC DATA OF A VIRTUAL S/P CROSSING A FR



UNIPOLAR configuration

Internal magnetic configuration II
(Mulligan et al. 1998)

perpendicular to Ecliptic Plane

Magnetic Cloud Type	WNE	ESW	ENW	WSE
Leading Field	West (-By)	East (+By)	East (+By)	West (-By)
Axial Field	North (+Bz)	South (-Bz)	North (+Bz)	South (-Bz)
Trailing Field	East (+By)	West (-By)	West (-By)	East (+By)
Helicity	RH	RH	LH	LH

Figure 2. Four flux rope model orientations highly inclined with respect to the ecliptic plane. Note N=north, S=south, E=east, W=west [after *Zhao and Hoeksema [1996]*].

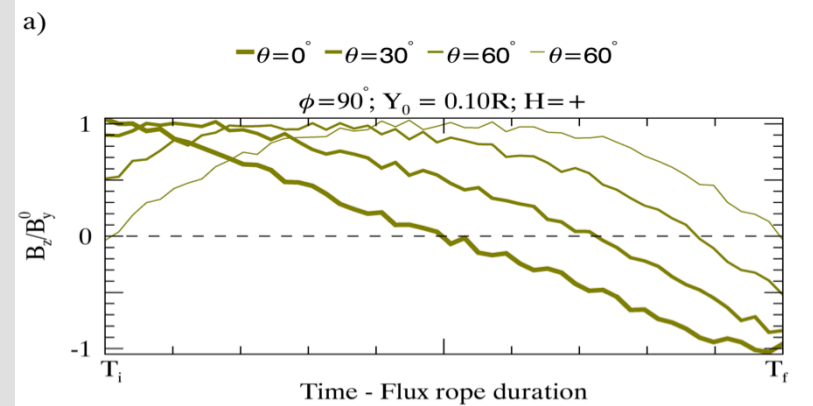
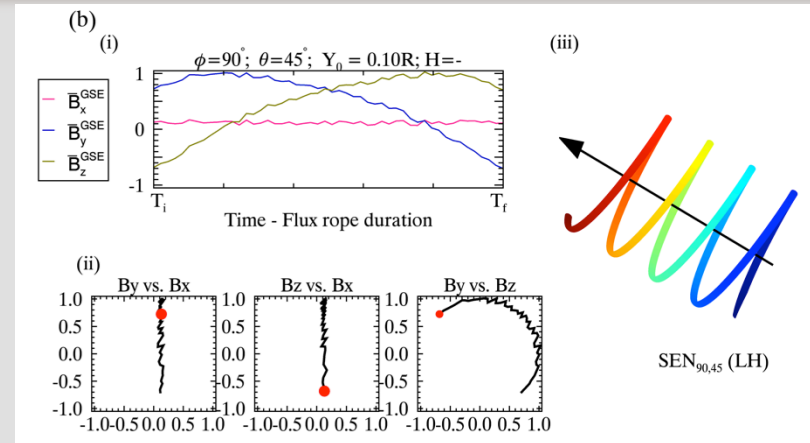
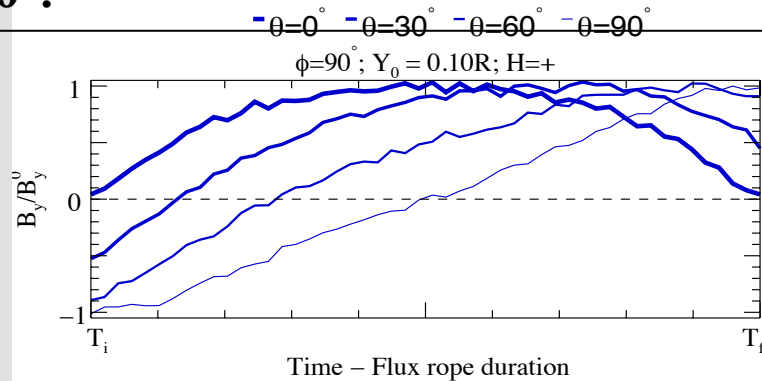
SYNTHETIC DATA OF A VIRTUAL S/P CROSSING A FR

What is the threshold between Bipolar and Unipolar?

$\theta = 45^\circ$ [Mulligan et al. 1998, Huttunen et al. 2005]

$\theta = 35^\circ - 55^\circ$ [Palmerio et al. 2018]

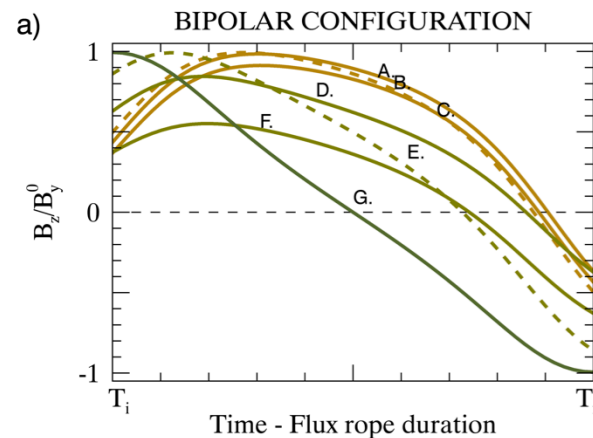
For a front ($\Phi=90^\circ$ or 270°) ICME -F the B_z changes in the polarity will be between 70% to 90% if the tilt (θ) is $30^\circ - 60^\circ$ a)



SYNTHETIC DATA OF A VIRTUAL S/P CROSSING A FR

For BIPOLAR configurations - Does the longitude matter?

Lepping & Wu, 2010



NORTH-TO-SOUTH (NS) Bz

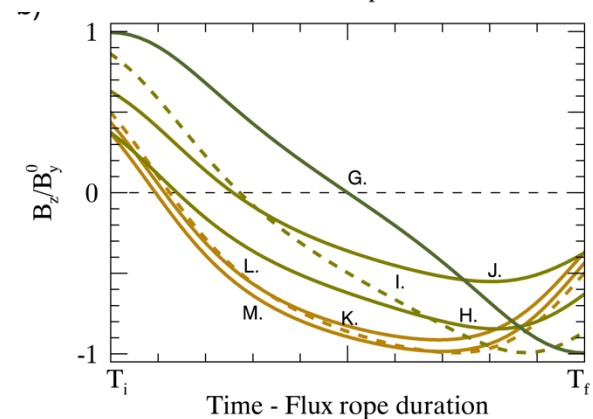
- A. ($\phi = 50^\circ, \theta = 60^\circ, H = +$) & ($\phi = 230^\circ, \theta = 60^\circ, H = -$)
- B. ($\phi = 90^\circ, \theta = 60^\circ, H = +$) & ($\phi = 270^\circ, \theta = 60^\circ, H = -$)
- C. ($\phi = 130^\circ, \theta = 60^\circ, H = +$) & ($\phi = 310^\circ, \theta = 60^\circ, H = -$)

↑ Mostly North

- D. ($\phi = 20^\circ, \theta = 30^\circ, H = +$) & ($\phi = 200^\circ, \theta = 30^\circ, H = -$)
- E. ($\phi = 90^\circ, \theta = 30^\circ, H = +$) & ($\phi = 270^\circ, \theta = 30^\circ, H = -$)
- F. ($\phi = 170^\circ, \theta = 30^\circ, H = +$) & ($\phi = 350^\circ, \theta = 30^\circ, H = -$)

- NS -

- G. ($\phi = 90^\circ, \theta = 0^\circ, H = +$) & ($\phi = 270^\circ, \theta = 0^\circ, H = -$)



NORTH-TO-SOUTH (SN) Bz

- G. ($\phi = 90^\circ, \theta = 0^\circ, H = +$) & ($\phi = 270^\circ, \theta = 0^\circ, H = -$)

- NS -

- H. ($\phi = 20^\circ, \theta = -30^\circ, H = +$) & ($\phi = 200^\circ, \theta = -30^\circ, H = -$)
- I. ($\phi = 90^\circ, \theta = -30^\circ, H = +$) & ($\phi = 270^\circ, \theta = -30^\circ, H = -$)
- J. ($\phi = 170^\circ, \theta = -30^\circ, H = +$) & ($\phi = 350^\circ, \theta = -30^\circ, H = -$)

↓ Mostly South

- K. ($\phi = 130^\circ, \theta = -60^\circ, H = +$) & ($\phi = 310^\circ, \theta = -60^\circ, H = -$)
- L. ($\phi = 90^\circ, \theta = -60^\circ, H = +$) & ($\phi = 270^\circ, \theta = -60^\circ, H = -$)
- M. ($\phi = 50^\circ, \theta = -60^\circ, H = +$) & ($\phi = 230^\circ, \theta = -60^\circ, H = -$)

Name	Description	Portions of Polarity
N	North	N[90-100]%, S[10-0]%
NSN	NS mostly N	N[70-90]%, S[30-10]%
NS	North-to-South	N[40-60]%, S[60-40]%
NSS	NS mostly S	N[10-30]%, S[90-70]%
S	South	N[0-10]%, S[100-90]%

Nieves-Chinchilla et al.
2018b, in preparation

QUESTIONS:


- ❑ What would be the in-situ mag observations for different s/p trajectories crossing a fR?
- ❑ How many display such expected fR signatures?



TO-DO LIST:

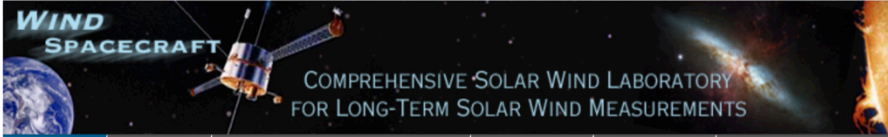
- ✓ Create synthetic data for all (enough) fR configurations to figure out.
- ✓ Check a large set of ICMEs with M0s and see how many display fR signatures

MODELING HELIOSPHERIC FLUX-ROPEs - WIND 1995 - 2015



NATIONAL AERONAUTICS
AND SPACE ADMINISTRATION

NASA Homepage
Goddard Space Flight Center
Sciences and Exploration Directorate



COMPREHENSIVE SOLAR WIND LABORATORY
FOR LONG-TERM SOLAR WIND MEASUREMENTS

WIND
Data
Instrument Descriptions
Orbit Info
Links
Bibliography

[< Back to home](#)

[1995 - 1996 - 1997 - 1998 - 1999 - 2000 - 2001](#)
[2002 - 2003 - 2004 - 2005 - 2006 - 2007 - 2008](#)
[2009 - 2010 - 2011 - 2012 - 2013 - 2014 - 2015](#)

Text filter:

Filter table:

None

Shock events only

Flux-rope only

Ejecta only

Wind ICME Catalogue

1995

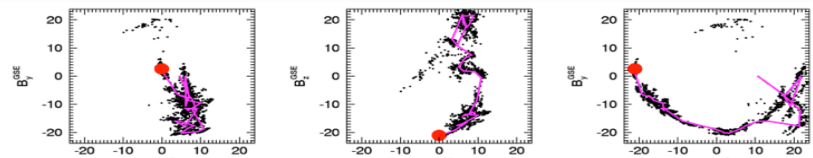
	ICME[1] start time	(Shock)	MOI[2] start/end time	FR/E[3]	MO start/end time	ICME end time	B[4]	V _{sw} [5]	V _{exp} [6]			H0[7]
1	1995 038 02/07 19:11	--	039 02/08 03:21	C	041 21:36	041 02/10 21:36	8.32	377	52	P	-	H0
2	1995 063 03/04 00:36	Y	063 03/04 11:23	F	064 03:07	064 03/05 03:07	10.82	443	10	P	F	H0
3	1995 065 03/06 02:11	--	065 03/06 07:11	F	066 02:23	066 03/07 02:23	8.24	458	-	P	F	H0
4	1995 093 04/03 06:43	--	093 04/03 12:45	F	094 13:26	094 04/04 13:26	8.92	295	37	P	F	H0
5	1995 095 04/05 07:11	--	095 04/05 17:59	F	096 17:16	096 04/06 17:16	7.30	332	-1	P	F	H0
6	1995 133 05/13 10:19	--	133 05/13 10:19	E	133 16:00	133 05/13 16:00	10.86	329	7	P	-	H0
7	1995 181 06/30 09:21	--	181 06/30 14:23	F	183 16:47	183 07/02 16:47	8.58	397	82	P	F	H0

<https://wind.nasa.gov/ICMEindex.php>

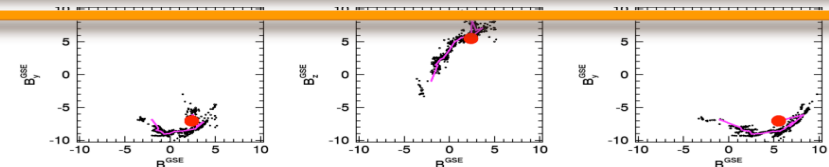
SORTING ICMES BY COMPARING WITH SYNTHETIC DATA

Criteria

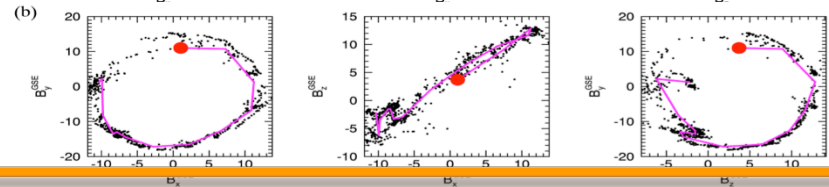
» F_r : Single rotation [90°-180°].
1995 October 18



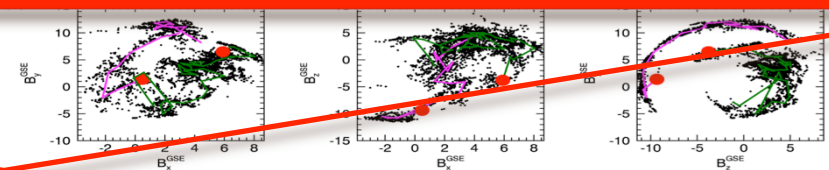
» F^- : Single rotation <90°.
2012 September 4



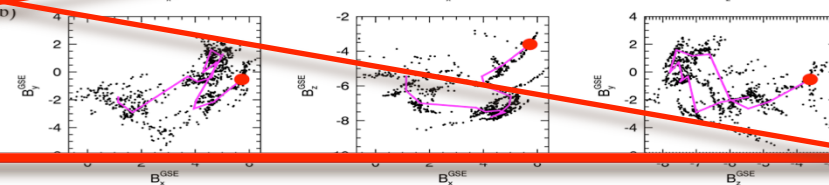
» F^+ : Single rotation >180°.
2006 September 6



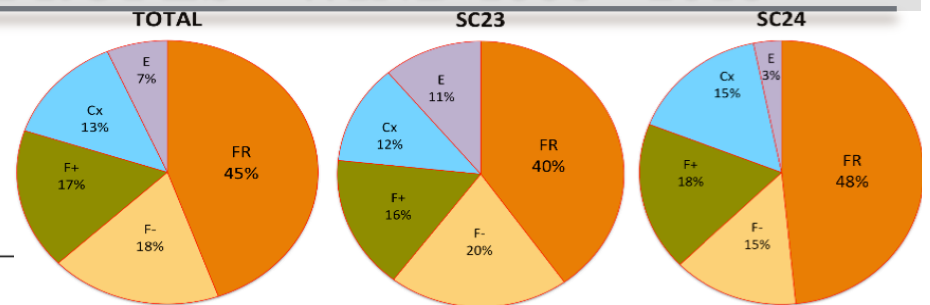
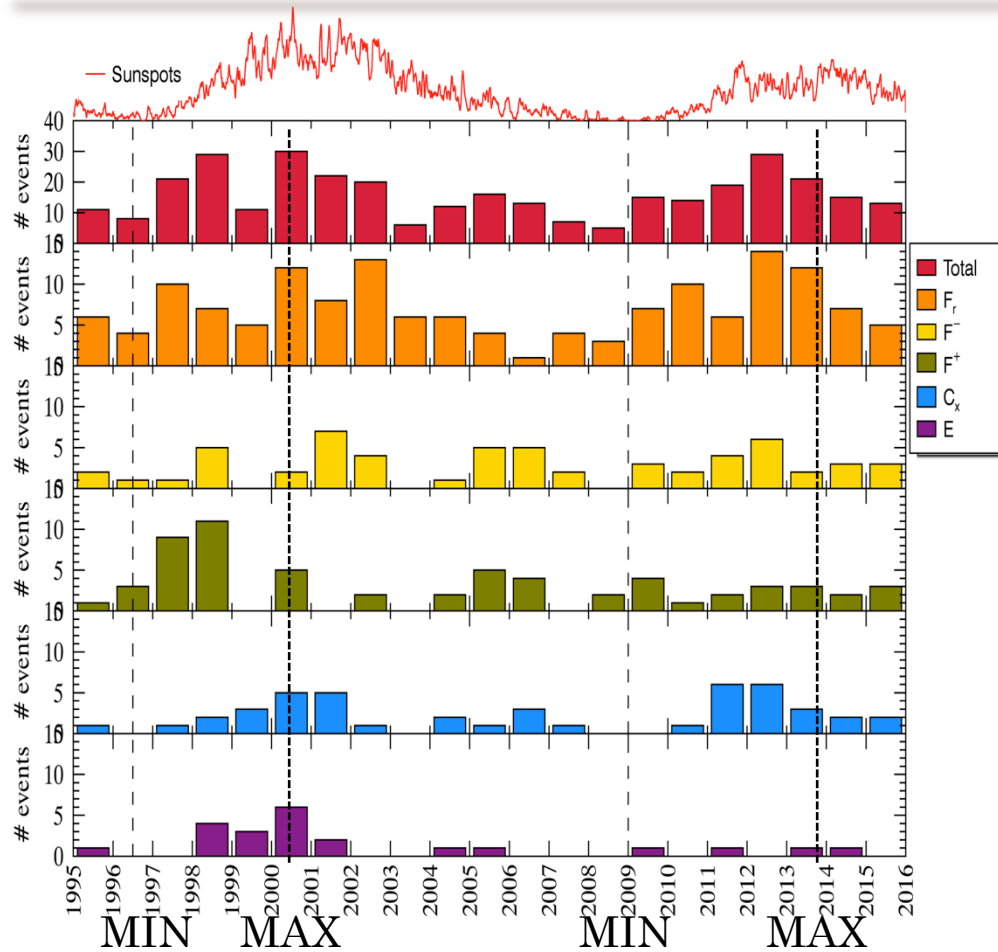
» C_x : Multiple rotations.
1995 February 7



» E : No-clear rotation.
1997 February 10



MODELING HELIOSPHERIC FLUX-ROPE - WIND 1995 - 2015



F → 80%

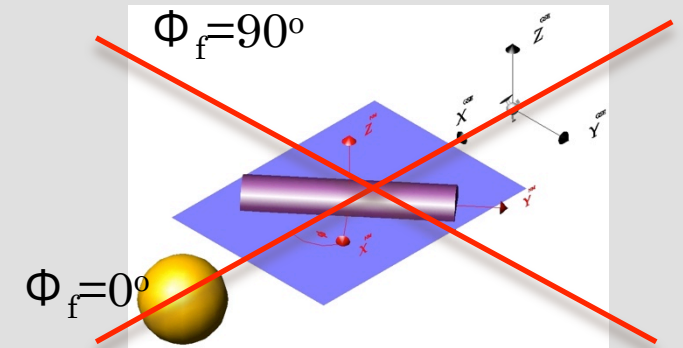
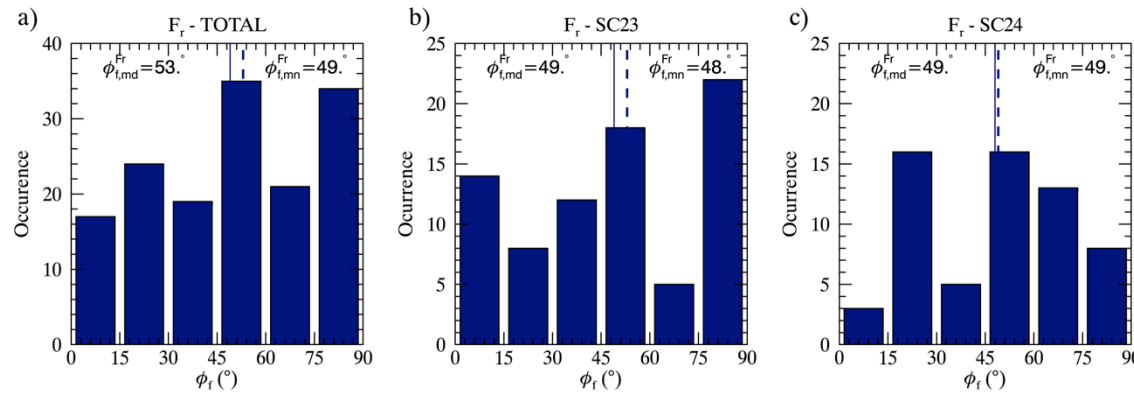
F → 76%

F → 81%

TOTAL [=337]	F [F_r, F^-, F^+]	Cx	E
TOTAL	270 [150,58,62]	45	22
SC23	153 [79,32,40]	24	17
SC24	102 [61,23,18]	20	4

1. ICMEs/MO & Fr follow the SC trend.
2. Maximum occurrence of Cx & E around SC maximums.

MODELING HELIOSPHERIC FLUX-ROPEs - WIND 1995 - 2015

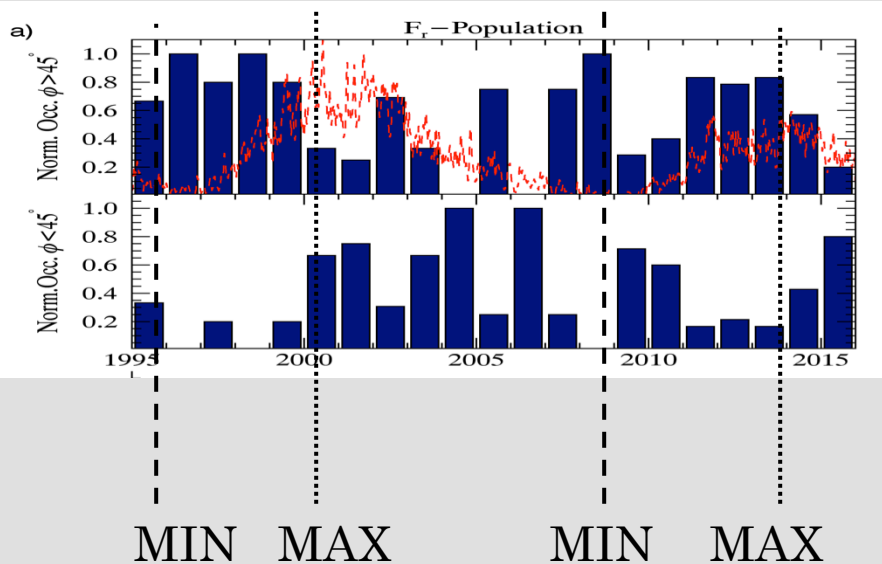


Longitude (ϕ) initially in the range from 0° to 360° , have been folded to a range from 0° to 90° . The new angle ϕ_f assesses if the flux rope axis is aligned ($\phi_f = 0^\circ$) or perpendicular ($\phi_f = 90^\circ$) to the observer (sun-earth line).

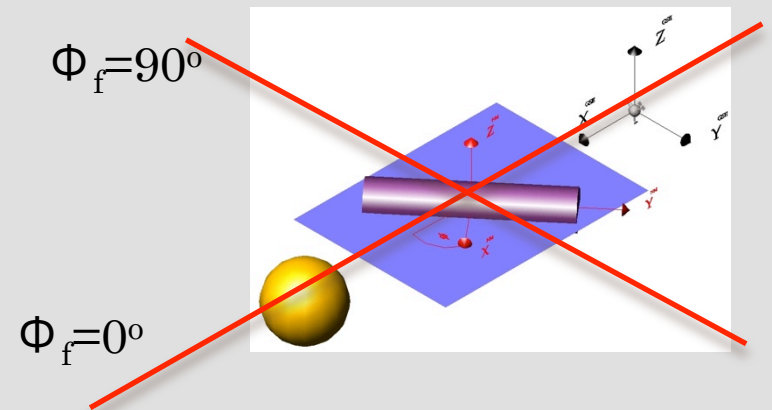
	P	TOTAL	SC23	SC24
$\phi_f > 45^\circ$	F_r	60.%	58.%	61.%

1. Visual inspection does not show any privilege in the axis longitude.
2. Quantitatively there is a slight tendency to be perpendicular to the observer.

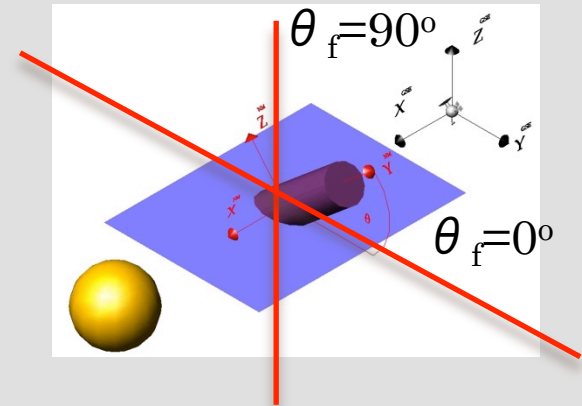
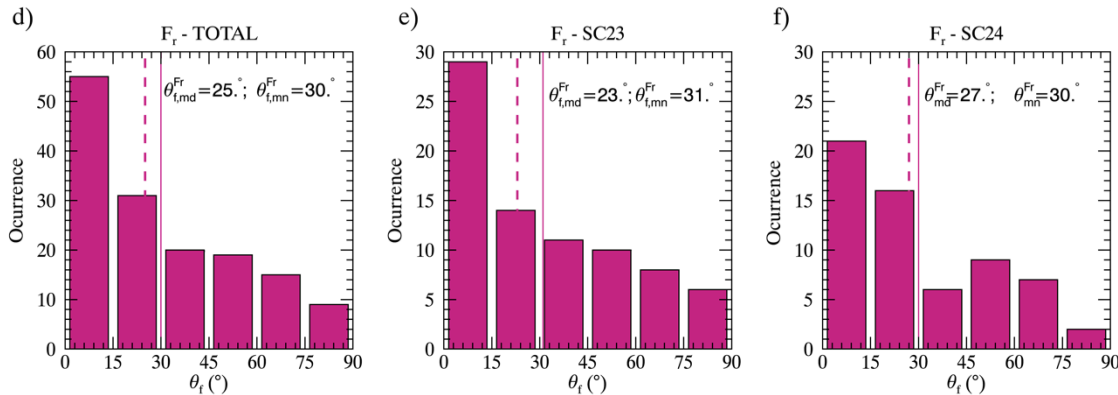
MODELING HELIOSPHERIC FLUX-ROPE - WIND 1995 - 2015



- During the rising phase of SC23 and SC24 the axis orientation is mostly perpendicular to the observer.
- Around SC23 maximum and declining phase towards SC24 minimum the axis orientation is mostly along to the Sun-Earth line.



MODELING HELIOSPHERIC FLUX-ROPEs - WIND 1995 - 2015

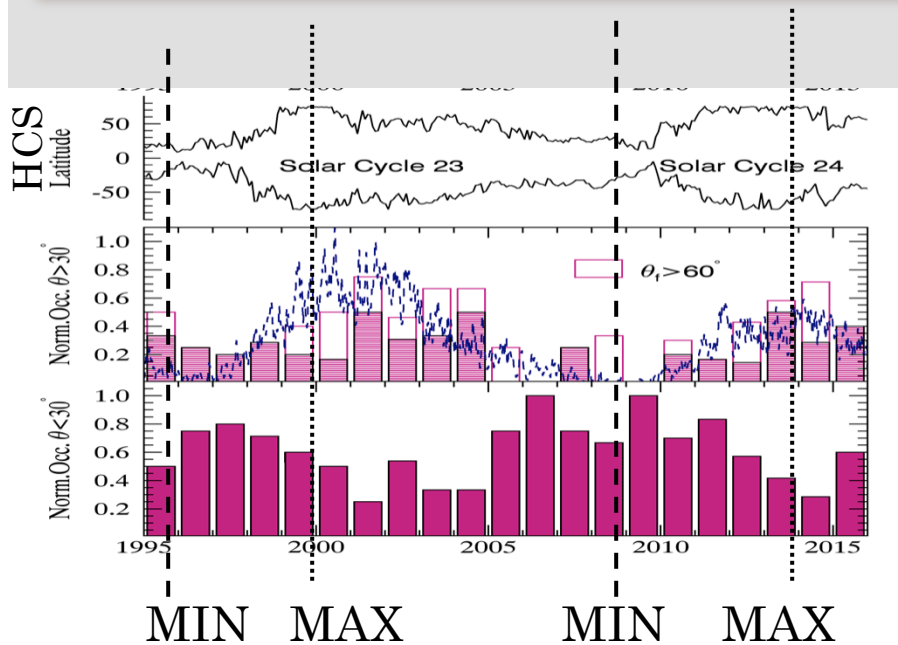


- Tilt(θ) initially in the range from -90° to 90° , have been folded to a range from 0° to 90° . The new angle θ_f assesses if the flux rope axis is on the ecliptic plane ($\theta_f = 0^\circ$) or perpendicular ($\theta_f = 90^\circ$) to the ecliptic plane.

	P	TOTAL	SC23	SC24
$\phi_f > 45^\circ$	F_r	60.%	58.%	61.%
$\theta_f < 30^\circ$	F_r	58.%	56.%	61.%

- Visual inspection shows a clear increase in the occurrence for the low tilted FRs ($\theta < 30^\circ$).
- Quantitatively more than 56% of the event are low tilted.

MODELING HELIOSPHERIC FLUX-ROPE - WIND 1995 - 2015



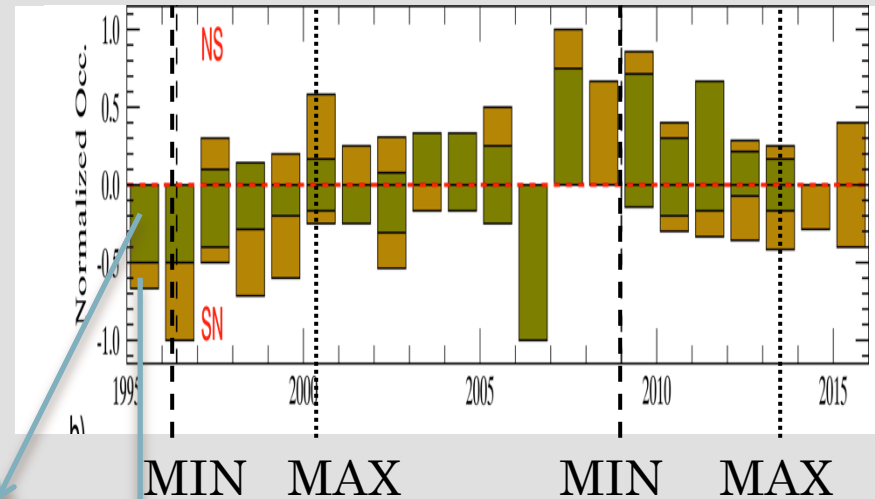
- Around maximum and mostly in the declining phase of SC23 and SC24 the occurrence of FR highly tilted are maximum, while the minimum and rising phase of SC23 and SC24 the FRs tilt are lowly tilted.
- There is ~20% of the events that remain low tilt depict of the background solar wind orientation.
- Inclination or tilt of the flux rope follow the SC trend and the HCS tilt. This result suggests that the solar wind orientation could affect to the CME orientation.

POLARITY

Comparing previous studies based on visual inspection [Li et al. 2011, 2014, 2018]:

- ✓ During the rising phase [Min to Max] the SN (SC23) configuration and NS (SC24) dominate.
- ✓ During couple of years around the minimum (couple of years) the events display exclusively SN or NS polarity.
- However, during the declining [Max to Min] phase there is not clear dominant configuration.

- ✓ There is a cyclic reversal of the bipolar magnetic field flux rope configuration



NS, or SN

[Hybrid] NSN, NSS, SNN, SNS

TAKE-AWAYS

1. Not every thing that glitters is a flux rope!!

- Flux ropes have a solar cycle (SC) dependence.
- ~80% of the ICME-MOs are flux ropes but just ~45% display signatures of 'pure' flux rope.
- Complex structures and Ejecta occurrence increases during the maximum.

2. The ICMEs configuration have a solar cycle dependence.

- The occurrence of the events with perpendicular axis to the observer increases during the rising phase of the SC.
- The occurrence of the events highly inclined increases during maximum and declining phase.

3. The flux rope polarity is not binary but diverse.

- Between the Bipolar [NS, SN] and Unipolar configurations there are Hybrid configurations [NSN, NSS, SNN, SNS] that we quantify and describe based on the longitude and tilt.
- There is a cyclic reversal of the bipolar magnetic field flux rope configuration.